SOME DYNAMICAL PROBLEMS IN CONTINUUM PHYSICS

A Tutorial Lecture

by

Millard F. Beatty
Department of Engineering Mechanics
University of Kentucky
Lexington, KY 40506

and

Institute for Mathematics and Its Applications
University of Minnesota
Minneapolis, MN 55455

May 1985

INTRODUCTION

This is a tutorial lecture[1] about some one and two dimensional dynamical problems in continuum physics. Three problems concerning the physical behavior of fluid and solid materials in a dynamical setting will be discussed. The first example is an old, but fascinating problem in the fluid mechanics of jet instability whose solution I will relate to a rather remarkable technological achievement by American industry. My discussion of this problem will demonstrate the gap in time between the creation of important physical and mathematical results and their conversion to useful technology.

Of course, not every important scientific or mathematical discovery in the physics of continua has the same potential for technological application. Nevertheless, basic results seem always to find relevant applications that bear on the advancement of technology by providing useful supportive information about the physical nature and mechanical behavior of materials. The other problems that I will discuss fall in the later category. These involve the dynamical response of highly elastic solid continua.

An interesting phenomenon produced in the transverse vibration of a rubber cord stretched over its entire limit of extensibility will be described both by experiment and theory. This analysis involves the superposition of small amplitude

---

1. This lecture was broadcast live on UNITE television from the University of Minnesota at Minneapolis on May 28, 1985.

oscillations on a finitely deformed equilibrium configuration of the string. The results will be related to the molecular structure of the rubber materials tested. Then we shall explore the finite amplitude, free longitudinal vibration of a body supported by a rubber spring. The exact solution of this nonlinear problem will be outlined, and its physical implications will be illustrated. Finally, the problem of small amplitude, free longitudinal oscillations superimposed on a finitely deformed axial stretch of the rubber support studied in the previous problem will be related to experimental data, some of which has application in human biology.

CHAPTER 1

APPLIED MATHEMATICS AND TECHNOLOGY

If one turns on a water faucet and then gradually reduces the flow rate from the spigot so that the flow is slow but steady, one usually will observe that the stream becomes unstable and disintegrates randomly into drops of irregular size, shape and spacing. Sometimes one may find that by whistling at a constant pitch near the stream, the induced vibration will enhance this readily observed jet breakup phenomenon and produce somewhat improved regularity in the drops. The general effect is shown in the series of stroboscopic photographs[2] in Figs. 1 to 4. The Figs. 2 and 3 are enlargements of the regions between the arrows indicated in Figs. 1 and 2, respectively; and Fig. 4 is a separate illustration of the ultimate jet disintegration.

1.1. Theory of the Fluid Jet Instability Phenomenon

This interesting instability behavior of liquid jets was first studied by several 19th century researchers. It was described in experiments by Bidone in 1830, Savart in 1833, and Magnus in 1859. It appears that Plateau, in 1873, was the first to show, both from theory and experiment, that because of surface tension, the principal cause of this instability phenomenon, the cylindrical shape of a jet of fluid in a steady flow is an

---

2. These photographs were provided by Professor C.F. Knapp, Department of Mechanical Engineering, University of Kentucky. I thank Prof. Knapp for their use in this report.

Fig. 1: Instability of a Fluid Jet

Fig. 2: Formation of the Stream into Drops

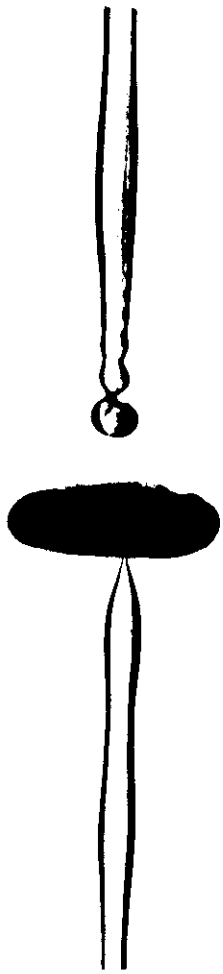

Fig. 3: Closeup of the Jet Disintegration into a Drop and a Possible Satellite Droplet Behind it.

Fig. 4: Disintegration of the Liquid Jet into Drops of Irregular Size, Shape and Spacing; and Appearance of Some Satellite Droplets.

unstable configuration of equilibrium whenever its length λ exceeds its circumference πd_j, as shown in Fig. 5. Thus, Plateau's criterion for the jet instability is that $\lambda > \pi d_j$.

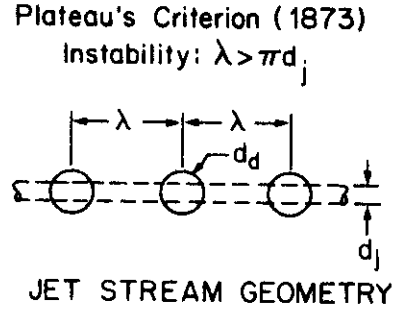

Fig. 5: Stream Geometry and its Uniform Breakup
The droplets in a uniform stream are spaced a distance λ apart. Each droplet of diameter d_d is composed of fluid previously contained in a fluid cylinder of length λ and diameter equal to the mean jet diameter d_j. See [3].

However, it was 1878 when the subject received a particularly elegant mathematical analysis at the hands of Lord Rayleigh [1-2]. A periodic pressure variation acting on the fluid jet produces undulation of its lateral surface. Surface tension effects act to induce jet instability where the jet stream is narrowest. Since the surface tensions become large where the curvature is high, they act to further reduce the stream diameter until the stream breaks into separate drops, as described above. Rayleigh showed that a superimposed small sinusoidal diametral

disturbance grows exponentially in time, as diagrammed[3] in Fig. 6, until eventually the stream breaks into droplets at the dis-

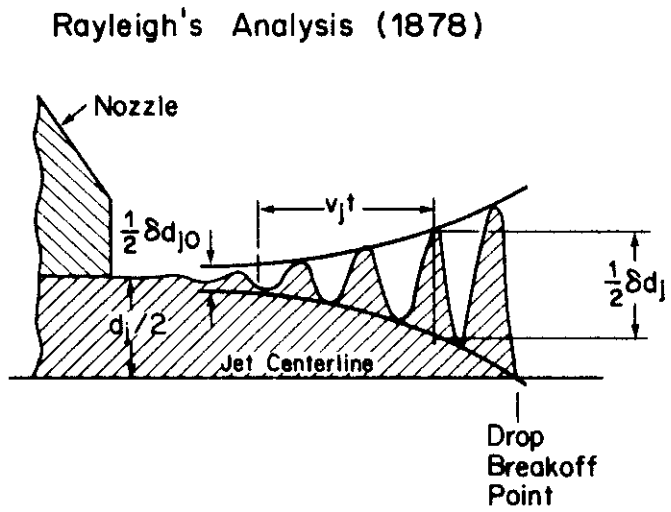

Fig. 6: Stream Instability of the Steady Flow of an Ideal Fluid Jet. See [3].

turbing rate. He found that the stream perturbation growth δd_j is given by

$$\delta d_j = \delta d_{j0} \exp\left[I(z) \left(\frac{8\sigma}{\rho d_j^3} \right)^{1/2} t \right] \qquad (1.1)$$

wherein d_j is the jet diameter, σ is the surface tension, ρ denotes the fluid density, δd_{j0} is the initial stream

---

3. Several of the illustrations herein are modified reproductions of figures that have appeared in IBM publications [3-4]. I thank Mr. W.L. Buehner of the Office Products Division of IBM for permission to reproduce these for educational use.

disturbance, and

$$I(z) \equiv \left[\frac{z\, I_0'(z)}{I_0(z)} (1 - z^2) \right]^{1/2} \quad \text{with } z \equiv \frac{\pi d_j}{\lambda} . \qquad (1.2)$$

Herein, $I_0(z)$ denotes the modified Bessel function of the first kind. The function $I(z)$, therefore, is the measure of instability, so it has been named the **instability factor** [4]. This measure is highly dependent upon the **stream factor** $k \equiv \lambda/d_j$, the ratio of axial drop spacing λ and jet stream diameter d_j described in Fig. 5. The instability factor is the measure of the ease with which a stream breaks up into uniformly spaced droplets. A plot of the instability factor as a function of the stream factor is shown in Fig. 7. Theoretically, below a stream

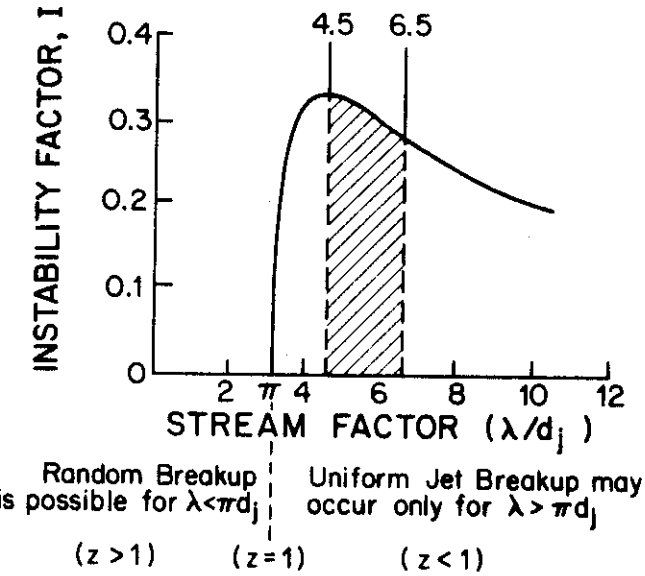

Fig. 7: Rayleigh's Instability Curve Showing that λ must Exceed the Stream Circumference before Uniform Breakup can Occur, and Showing the Optimum Jet Instability at the Stream Factor $\lambda/d_j = 4.5$. See[3].

factor of π, that is, for $k = \lambda/d_j < \pi$, we have $z > 1$ in (1.2) and only random stream breakup may occur. Therefore, in order that $z < 1$ may hold in (1.2), the length λ must exceed the stream circumference πd_j before uniform breakup can occur. Hence, Plateau's criterion for jet breakup falls out naturally from Rayleigh's analysis. But there is more. According to Rayleigh's calculation, as shown in Fig. 7, the maximum instability occurs at a stream factor of 4.51, after which the instability gradually decreases. This extreme is the value of the stream factor at which the jet disintegrates with greatest ease into droplets of uniform size and spacing; it characterizes the optimum condition for jet instability. Experiments [3] confirm that the best operating range for stable, satellite-free drop formation occurs between stream factors of 4.5 and 6.5, as indicated in Fig. 7. Hence, the stream factor introduced by Rayleigh turns out to have critical importance in the formation of stable, satellite-free drops. We shall see further on why this is significant.

1.2. A Technological Application of Rayleigh's Analysis

In 1965, Richard G. Sweet of Stanford University showed that an electrical charge could be impressed on the drops that form out of a jet of electrically conducting ink [5]. He discovered that even when the drops were generated at the rate of 100,000 or more per second, the charge on each drop could be determined independently so that the trajectory followed by each could be controlled by passing them through a uniform electric field. His interest was in the construction of a high speed oscillograph

for recording rapidly changing electrical signals on a moving strip chart. Hence, Sweet had in mind the application of Rayleigh's theory of jet instability to electronically controlled graphics. In modern terms, this would be identified as a form of **computer graphics**.

1.2A. A Technological Achievement

The same technique has found use in other applications, such as the sorting of cells in blood specimens, the atomization of fuels, and in the printing of alphabetic characters, which Sweet himself was among the first to investigate [6]. To get a feel for the performance speed in Sweet's printer application, let us estimate that the drops are formed at a rate of 100,000 per second and that an alphabetic or other character is composed of 100 drops. Then the maximum printing rate in Sweet's device would be roughly 1,000 characters per second. Of course, actual rates would be much slower because not every drop in the jet stream can be used. Nevertheless, it appears reasonable that rates of nearly 100 characters per second could be readily obtained in a practical printer without the use of high speed mechanical impact printing elements, well-known for their inherent problems of wear, fatigue and typical acoustical noise generation. A business office printer of this kind was first developed by the A.B. Dick Company; but I know nothing of its description, nor when it was first produced.

In 1976, however, these theoretical and experimental developments culminated in a remarkable modern technological

achievement when the Office Products Division of IBM at Lexington, Kentucky, released a new version of the ink jet printer which was capable of producing character images of typewriter quality [7]. The ink jet printer, which is illustrated schematically in Fig. 8A, produces an image from tiny spherical droplets of electrically charged ink, approximately

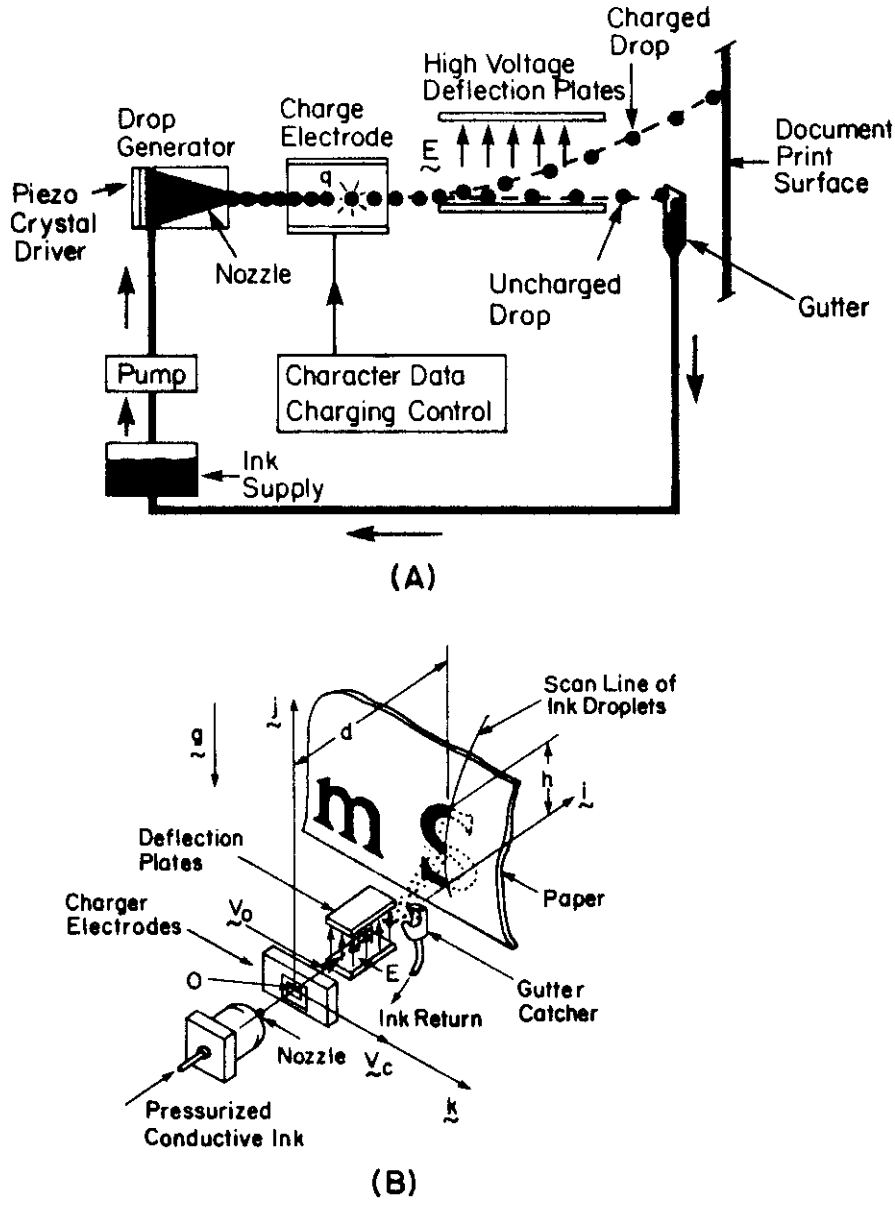

Fig. 8: Schema of the IBM Ink Jet Printing Process. See [4].

30μ m (~1/1000 in) in diameter, fired from a drop generator orifice the size of a human hair. Ink is pumped from its reservoir into the drop generator wherein a synchronizing signal induced by the vibrations of a piezoelectric crystal creates drops uniform in size, velocity and spacing at the synchronizing frequency rate of 117,000 drops per second. The periodic pressure variation applied by the crystal produces undulation of the lateral surface of the jet stream, and surface tension effects cause the stream to breakup into droplets, in accordance with Rayleigh's theory, as described before. The disintegrating ink jet then passes between charging electrodes where the conducting drops are selectively charged electrostatically following instructions from programmed electronic control circuits that describe the image characters in terms of charge-no charge language. Moving at about 40 mph (730 in/sec) initially, the charged droplets pass through a constant electric field that directs them onto the paper. While the vertical scanning occurs, a control mechanism moves the printer carriage parallel to the paper at a constant speed of 7.7 in/sec, i.e. fast enough to traverse a standard page width in about one second. In this way, the ink jet printer composes about 80 characters each second, that is to say, a full line of type across an 8 $^{1}/_{2}$ inch page in about one second or less.

1.2B. The Working Principle of the Ink Jet Printer

To perceive the working principle of the ink jet printing operation, we may consider a fluid droplet P of mass m and charge

q given an initial velocity $\underset{\sim}{v}_0 = v_0\underset{\sim}{i}$ relative to the printer carriage, as illustrated in Fig. 9. To simplify the analysis, we may ignore aerodynamic drag and wake effects, and the influence of electric repulsive forces between droplets. Then the total force acting on the drop is the constant force due to its weight $\underset{\sim}{W} = -mg\underset{\sim}{j}$ and the applied electric field force $\underset{\sim}{F}_e = q\underset{\sim}{E} = qE\underset{\sim}{j}$. Thus, the equation of motion $\underset{\sim}{W} + \underset{\sim}{F}_e = m\underset{\sim}{a}(P,t)$ yields the following motion for the trajectory of P:

$$\underset{\sim}{x}(P,t) = \frac{1}{2}(cE - g)t^2\,\underset{\sim}{j} + v_0 t\,\underset{\sim}{i}. \qquad (1.3)$$

That is, the droplet path is the parabola

$$y(x) = \frac{1}{2v_0^2}(cE - g)x^2 \quad \text{with} \quad c \equiv q/m. \qquad (1.4)$$

Let us suppose for simplicity that the deflection plates of length d extend from the origin at the charger to the paper surface, as suggested in Figs. 8B and 9. Then (1.4) holds

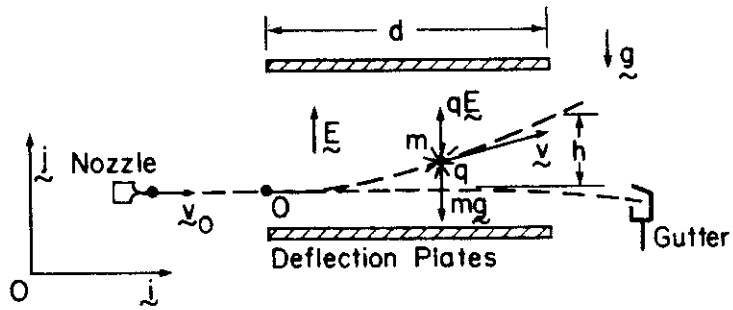

Fig. 9: Working Principle of the Ink Jet Printer. See [19].

for $0 \leq x \leq d$. Hence, at $x = d$, the droplet deflection or scan height $h = y(d)$ at the paper surface is determined by

$$h = \frac{d^2}{2v_0^2}(cE - g). \qquad (1.5)$$

The result shows that when an electrostatically charged drop enters the uniform electric field, the electric force alters its free fall trajectory and deflects it vertically by an amount proportional to its charge. An uncharged drop passes straight through the field in free fall and is captured by a gutter catcher that returns the unused ink to its reservoir, as illustrated in Figs. 8 and 9. A charged drop strikes the paper. The alphabetic or any other characters are formed by directing the ink drops onto the paper in proper overlapping patterns determined by the printer electronics. An example [4] is shown schematically in Fig. 8B. The decision to charge or not to charge is made automatically 117,000 times each second. The formula (1.5) shows that the character height is inversely proportional to the square of the stream speed v_0 which, in turn, is a function of the pump pressure. The printer controls the character height automatically by its pump control circuit. Some interesting style effects may be produced by varying the printer carriage rate. In this way, the ink jet printer is able to generate rapidly characters of typewriter quality.

A remarkable stroboscopic microphotograph of drops of ink

emerging from an ink jet printer is reproduced[4] in Fig. 10. A jet of ink that originated in the drop generator to the right has dissociated into equally spaced drops. The lower line of drops were not charged, so these are moving toward the ink gutter to the left. The larger gaps between the uncharged drops are the vacated positions formerly occupied by the field deflected charged drops that are travelling on trajectories above.

Fig. 10: Stroboscopic Microphotograph of Ink Drops in a Jet Printer.

---

4. This illustration first appeared on the cover of the Number 1 issue of the 1977 IBM Journal of Research and Development. See [4].

The Mead Corporation has built a high speed printer that uses some 600 nozzles lined up across the width of a page, and paper is drawn continuously under these [6]. (See Fig. 11.) An entire line of drops is formed at one time, and, as consequence, the Mead printer is capable of printing 45,000 lines per minute, but with low resolution. We have all seen some printed matter produced in this way; indeed, this kind of high speed printing has received wide application in the printing of junk mail. I understand that a high resolution device has been investigated by IBM. I don't believe the purpose is to improve the printed quality of our junk mail. Rather, with improved resolution, it may be possible eventually to print newspapers and magazines by ink jet printer graphics.

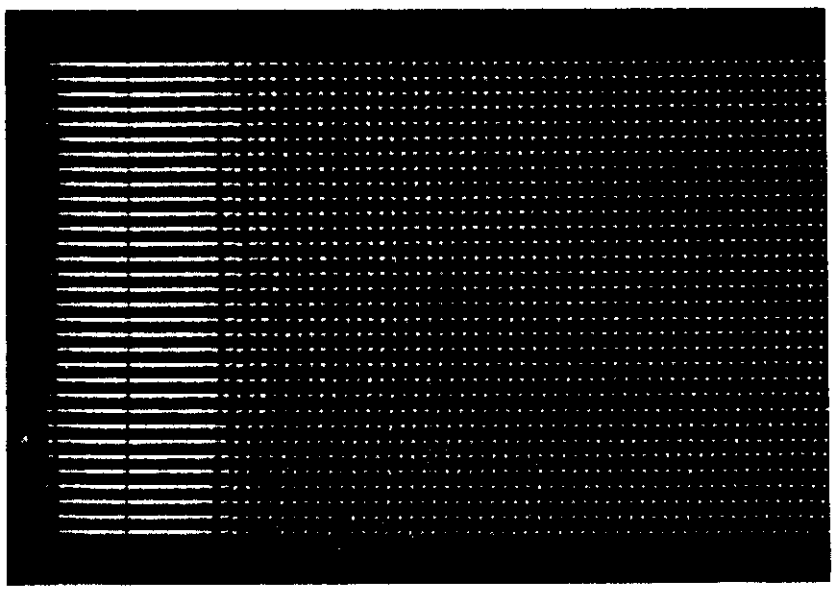

Fig. 11: Ink Jet Magnification Showing Multiple Streams of Ink Drops Emerging from the Left. Note the Uniformity in the Drop Size, Spacing and Speed. See [6].

1.2C. An Open Mathematical Problem in Ink Jet Technology

One may ask if there may be any open mathematical problems associated with this technology. I believe that possibly there may be many; but there is one, in particular, that I will mention briefly that may still constitute an unsolved problem and which may present a challenge for an applied mathematician or engineering scientist. This concerns the formation of smaller satellite droplets between the desired drops [3, 4, 6], as shown in Fig. 12A. These are troublesome because they can contaminate the deflection apparatus or cause misplaced marks on the printed document. The linearized stability analyses by Rayleigh and

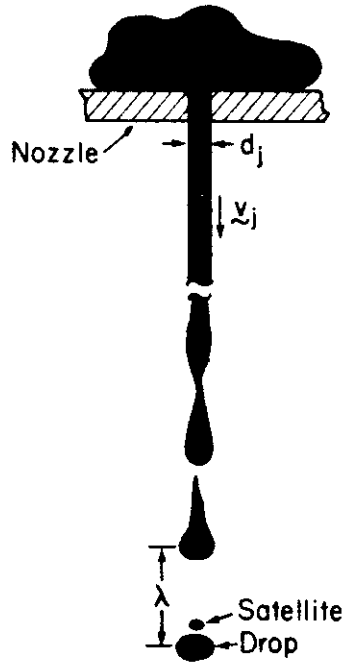

(A) Irregular Stream Breakup with Satellite Formation

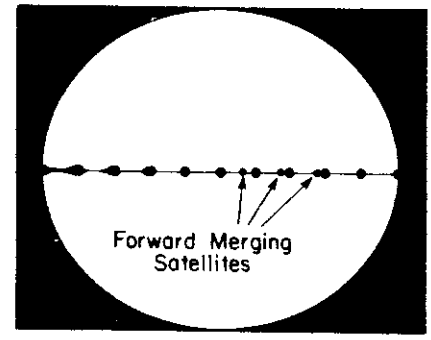

(B) Drawing of a Stroboscopic Micrograph of a Fluid Jet Showing Forward Merging (Fast) Satellites. Rear Merging (Slow) Satellites may also occur.

Fig.12 Jet Sream Breakup Showing the Formation of Satellite Droplets which may Contaminate the Deflection Apparatus and cause Misplaced Marks on the Printed Document. See [3,4].

others do not predict satellite droplet formation. Certain nonlinear instability studies [8], on the other hand, have revealed the existence of satellites along with the main drops. Unfortunately, the nonlinear analysis predicts simultaneous satellite separation at both ends of a main drop, and this stands in contradiction with experimental observations described schematically in Fig. 12B. A successful analysis of this problem could lead to a better understanding of drop generation and improved drop generator design.

Let us now turn to a class of interesting problems in solid continuum mechanics. The first example will relate the molecular structure of rubber to the vibrations of a rubber cord. The second will treat the finite amplitude oscillations of a mass suspended by a rubber spring; and the final example will relate some of these ideas to a small amplitude oscillation study that has an application in life science.

CHAPTER 2

MOLECULES AND THE VIBRATIONS OF A RUBBER CORD

When a rubber band is stretched sufficiently between the fingers of both hands, held close to the ear and plucked like a string of a musical instrument, it is observed that the pitch of the sound will vary only slightly as the stretch is increased. The first experimental investigations of this phenomenon were reported independently at the turn of this century by two scientists, T.J. Baker in Great Britain [9] and V. von Lang in Germany [10]. But neither provided a consistent theoretical explanation of the phenomenon. Of course, at that time, the mathematical theory of rubber elasticity had not yet been developed. Since the early 1940's, however, theoretical understanding of the mechanical properties of rubber has grown substantially, and we are now able to evaluate more accurately the substance of the Baker-von Lang observations. Let us begin by recalling Taylor's basic frequency formula.

2.1. The Transverse Vibrational Frequency of a String

Let us consider a homogeneous and perfectly flexible string that is stretched and fixed at both ends. If the string is plucked in the middle with a small displacement so that the transverse motion is planar, then the frequency ν of the fundamental mode of the transverse vibration of the string is given by Taylor's universal formula [11]:

$$\nu = \frac{1}{2\ell}\left[\frac{T}{m}\right]^{1/2}, \qquad (2.1)$$

where ℓ is the stretched length between the clamped ends, T is the constant string tension, and m is the mass per unit length ℓ of the string. Since the string is homogeneous, its total invariant mass is $M = m\ell$. If ℓ_o is the initial unstretched length of the string, then $\ell = \ell_o\lambda$, as shown in Fig. 13; and (2.1) may be rewritten as a function of the amount of stretch λ:

$$\nu(\lambda) = \frac{1}{2\ell_o}\left[\frac{T(\lambda)}{m_o\lambda}\right]^{1/2} \qquad (2.2)$$

in which $m_o = M/\ell_o$ is the mass per unit length ℓ_o and the function $T(\lambda)$ is determined by the constitutive equation of the material. Of course, the stretch $\lambda = \ell/\ell_o$, as indicated in Fig. 13, is a measure of the deformation of the cord.

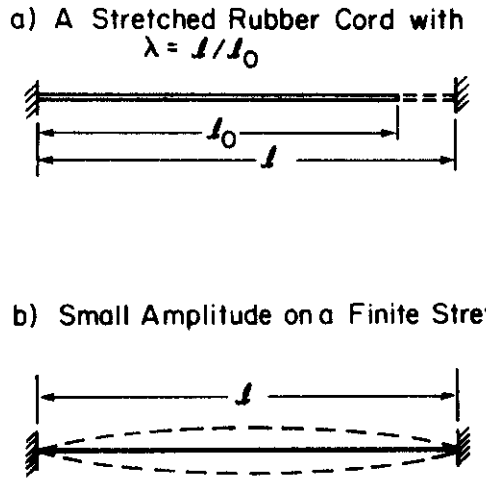

Fig. 13: The Transverse Vibration of a String Stretched an Amount $\lambda = \ell/\ell_0$

2.2. The Experimental Results

A low intensity laser beam apparatus was devised to determine the elastic properties of rubber by measurement of the small transverse vibrations of a rubber cord subjected to stretch varying to the maximum extension [12]. The apparatus is shown in Fig. 14. The experimental results are shown in Fig. 15. The Baker-von Lang phenomenon is evident for all of the rubber materials studied. It is seen that the frequency rises rapidly at first, but after a stretch of roughly 2, the curve flattens considerably so that subsequent growth in the frequency is small. This is consistent with our earlier description of the response. But what is the source of the phenomenon?

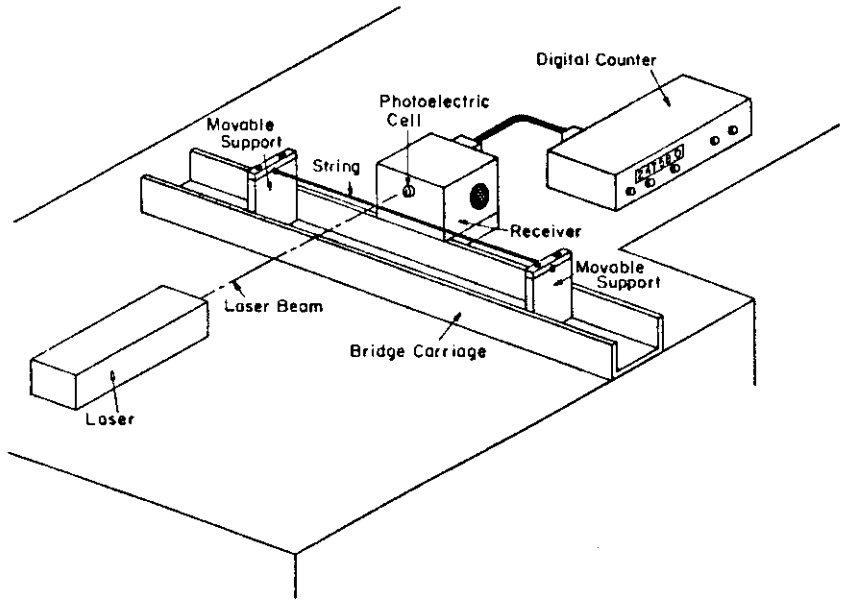

Fig. 14: Experimental Apparatus for the Frequency Test. See [12].

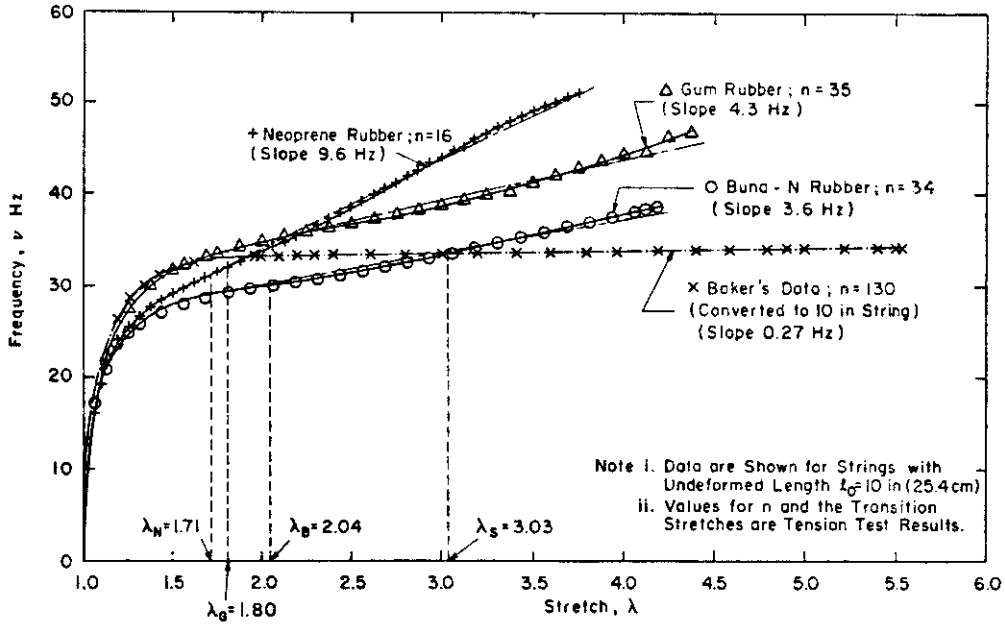

Fig. 15: Experimental Values of the Transverse Frequency vs. Stretch Averaged from Four Tests on Each of Three Rubber Materials and from Estimates of Baker's Data all for Strings with initial Length ℓ_0=10 in (25.4 cm). See [12].

2.3. The Theoretical Results

It is now well-known that rubber consists of molecules connected in tangled chains. This chain structure is what gives rubber its highly elastic properties, and several theoretical models that account for this hyperelastic behavior have been developed [13]. Beatty and Chow [12] found that the nearly constant pitch of a sufficiently stretched rubber band is predicted in slightly different ways by three theoretical models studied. Only two of these models will be described here; one of them shows directly how the number of links in the molecular chain structure affects the extensibility of rubber. These results are presented next.

2.3A. The Neo-Hookean Model of Rubber Elasticity

A neo-Hookean material model is an incompressible, isotropic elastic material for which

$$T(\lambda) = \frac{A_o E}{3}\left(\lambda - \frac{1}{\lambda^2}\right). \qquad (2.3)$$

Here A_o denotes the undeformed cross-sectional area of the cord and E is Young's modulus. This is the simplest model of rubber-like behavior; it derives from the Gaussian statistical mechanics of a molecular network [13].

Use of (2.3) in (2.2) yields the theoretical formula for the transverse vibrational frequency of a neo-Hookean rubber band:

$$\nu(\lambda) = \nu_\infty \left[1 - \frac{1}{\lambda^3}\right]^{1/2} \quad \text{with} \quad \nu_\infty \equiv [A_o E/12M\ell_o]^{1/2}. \qquad (2.4)$$

The graph in Fig. 16 of the frequency ratio ν/ν_∞ as a function of stretch shows clearly that the frequency rises rapidly as the cord length increases to about two or threefold, but with further extension the frequency remains almost unchanged [12]. Moreover, the phenomenon is a finite extensibility effect and may be attributed to the almost linearly elastic behavior of the material at large values of the stretch. Indeed, (2.4) gives $\nu/\nu_\infty > 0.98$ for $\lambda \geq 3$; and in this case the tension (2.3) is within 11% of being linear in λ. Thus, when a rubber band characterized by (2.3) is stretched sufficiently between the fingers of both hands and plucked, the pitch will vary only

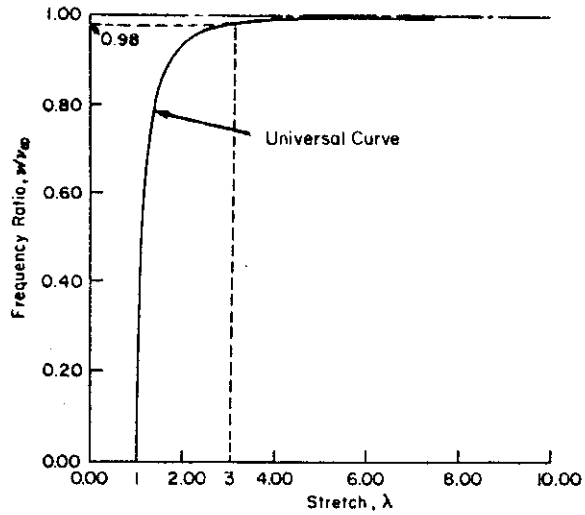

Fig. 16: The Frequency Ratio ν/ν_∞ is a Universal Function of λ: it is the Same for Every Neo-Hookean Material. See [12].

slightly while approaching a limit value $(2.4)_2$ as the stretch is increased. Therefore, our theoretical result for a neo-Hookean material supports and explains accurately the observations of Baker [9]. Notice that the frequency ratio ν/ν_∞ in (2.4) is a universal function valid for every neo-Hookean material. Of course, other constitutive models may yield similar though somewhat variable behavior.

2.3B. The James-Guth Model

This theory of isotropic rubber elasticity is derived from statistical considerations based upon a finitely extensible, long chain molecular network model. The relation between the tension and the stretch for this theory was first obtained by James and Guth in 1943 [14]; they derived the complex relation

$$T(\lambda) = \frac{CA_o}{3}\sqrt{n}\left[L^{-1}\left(\frac{\lambda}{\sqrt{n}}\right) - \lambda^{-3/2} L^{-1}\left(\frac{1}{\sqrt{\lambda n}}\right)\right] \text{ with } \sqrt{n} > \lambda \geq 1, \tag{2.5}$$

where n is the average number of links in a molecular chain, C is a material constant and $L^{-1}(y)$ is the inverse Langevin function defined by

$$L^{-1}(y) = x \text{ with } y = L(x) \equiv \coth x - \frac{1}{x}. \tag{2.6}$$

Notice that (2.5) shows that for this model the maximum network extensibility is less than $\sqrt{n}$. The constant C is related to Young's modulus in a complicated way which is of no concern here.

It seems intuitively clear that the ultimate extensibility of a chain, i.e. the ratio of the fully extended length between chain ends to the distance between chain ends in the natural state, increases with the number of its links. Therefore, the number n, as emphasized in (2.5), is a material parameter that characterizes the degree of elastic extensibility of the rubber material. As n grows indefinitely large, the formula (2.5) reduces to the neo-Hookean case.

Use of (2.5) in (2.2) delivers the transverse vibrational frequency of a rubber string characterized by the James-Guth model:

$$\nu(\lambda) = \nu_\infty \left[\frac{\sqrt{n}}{3\lambda}\left(L^{-1}\left(\frac{\lambda}{\sqrt{n}}\right) - \lambda^{-3/2} L^{-1}\left(\frac{1}{\sqrt{\lambda n}}\right)\right)\right]^{1/2} \tag{2.7}$$

for $1 \leq \lambda < \sqrt{n}$. Herein, by definition,

$$\nu_\infty = \frac{1}{2}\left[\frac{CA_o}{M\ell_o}\right]^{1/2}. \tag{2.8}$$

In view of the convexity of the inverse Langevin function, it can be shown that the transverse vibrational frequency for the James-Guth model is a monotonically increasing function of λ. The theoretical result (2.7) is shown in Fig. 17 for some typical values of n.

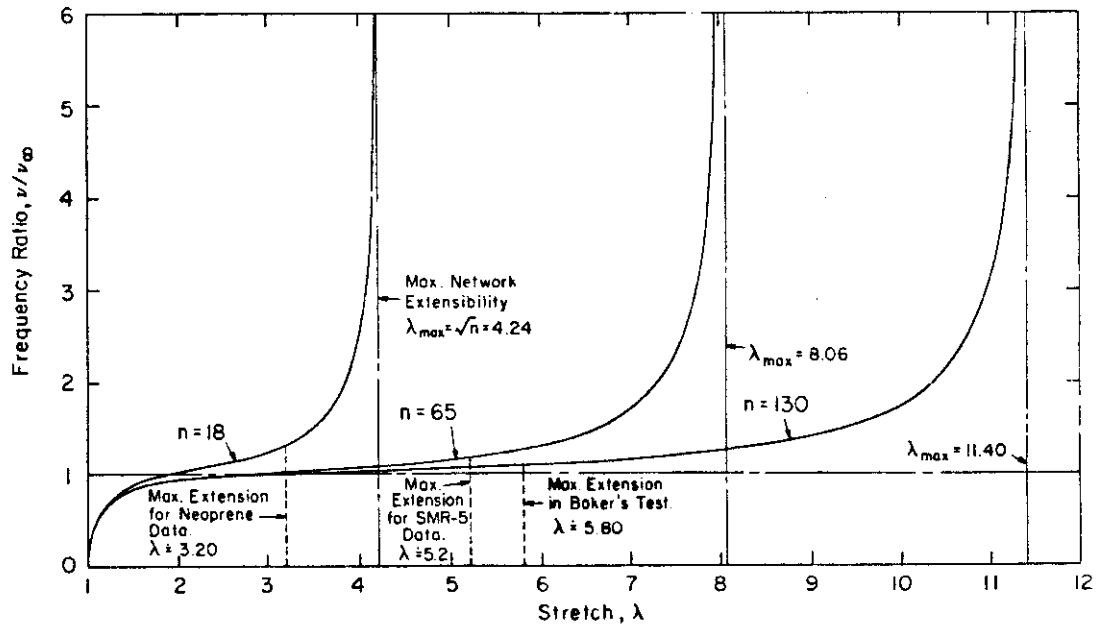

Fig. 17: Frequency Ratio vs. Stretch for a James-Guth String for Some Typical Values of n. See [12].

Unlike the previous two cases, as λ increases but remains bounded above by $\sqrt{n}$, the frequency does not approach a constant limit; rather, the frequency grows indefinitely as $\lambda \to \sqrt{n}$. Nonetheless, there exists a fairly straight intermediate range R in the neighborhood of the intercept $\nu(\lambda_o) = \nu_\infty$ at $\lambda = \lambda_o$ such that the frequency increases but little as λ increases through R. The extent of R, as seen from Fig. 17, depends on n. In this fairly flat range the frequency response is consistent with the characteristics of the Baker-von Lang phenomenon as described previously in the experiments by Beatty and Chow [12].

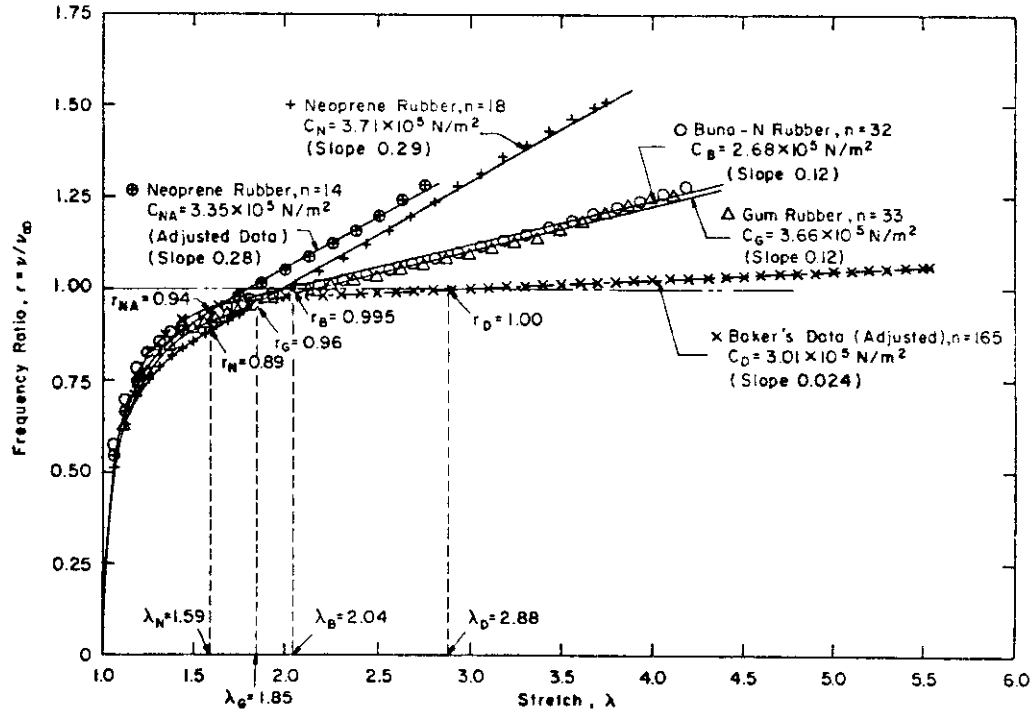

Fig. 18: Normalized Frequency Ratio vs. Stretch for Data Averaged From Four Tests on Each of Three Rubber Materials and for Estimates of Baker's Data. See [12].

The vibrating string data mentioned before were studied on the basis of this molecular model. A computer program was devised to determine simultaneously from the data the constant C and the apparent number of links n in the molecular chain structure of each of several varieties of rubber strings. The final result is summarized in Fig. 18. Notice that the gum and buna-N rubbers have almost the same apparent number of links n but different C values, and these curves coincide as predicted by (2.7), within expected experimental differences.

The experiments confirm that the nearly constant pitch phenomenon is a molecular network finite extensibility effect. It was observed for all the materials studied that after the stretch has about doubled, the frequency increases only very slightly as the tension is increased; and this slight rate of growth of the pitch is smaller for those rubbers for which the apparent number of chain links in the molecular network is larger. We shall see further on an important connection of these data with the results of the following problem of longitudinal oscillations [15-16].

CHAPTER 3

LONGITUDINAL VIBRATIONS OF A MASS ON A RUBBER SPRING

Various kinds of rubber spring mountings are used as suspension or compression supports for machines where only small amplitude oscillations commonly are encountered. Consequently, it is no surprise that in vibration analyses the affect of the nonlinearly elastic behavior of the rubber material has been ignored, even though the initial static deformation of the springy body may be substantial. It is easy to show that the undamped small amplitude, free vibration of a mass superimposed on a finite static extension or compression of an ideal, rubber spring leads to a simple harmonic solution for the attached load, but the fundamental frequency of the vibrations will depend upon the initial deformation. Hence, even in this case considerable error may be introduced into dynamical measurements of mechanical properties when the initial deformation is ignored; and the opportunity to discover other interesting results may be lost.

The exact solution for the undamped, finite amplitude free oscillations of a heavy mass supported vertically by a rubber suspension spring made of an ideal neo-Hookean material will be described next. We wish to determine the frequency (or the period) and to characterize the amplitude of the vibration.

3.1. Finite Oscillations of a Mass on an Ideal Rubber Spring

Everyone probably has seen a child's paddle ball toy which is sketched in Fig. 19. There is no doubt that the motion of the

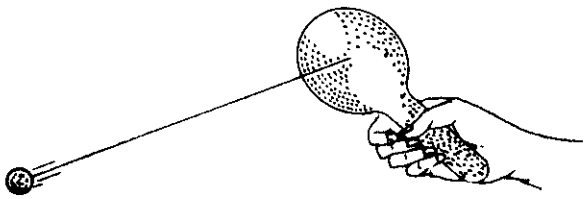

SOLITARY TENNIS GAME
"PADDLE BALL"

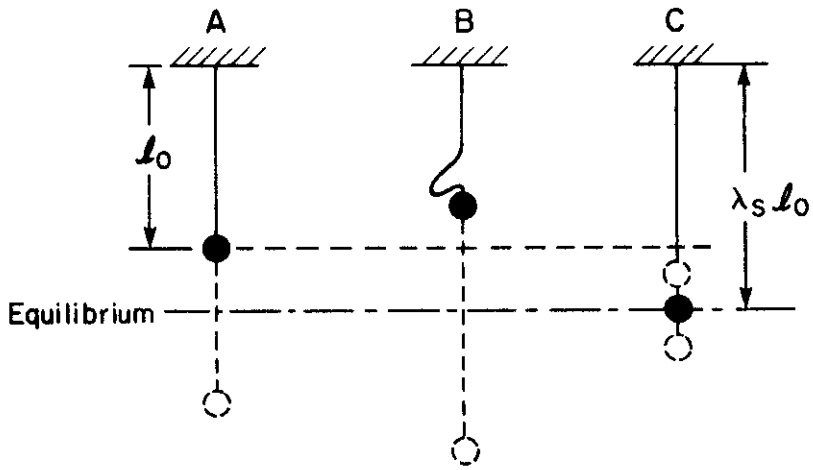

Fig. 19: Finite Amplitude Oscillations Related to a Paddle Ball Toy.

A. Finite Amplitude, Free Vibrations with Pure Stretch

B. Finite Amplitude, Free Vibrations with Free Flight

C. Small Amplitude, Free Vibrations with Static Stretch

ball, which is attached to the end of a highly elastic rubber string, executes finitely large amplitude oscillations. Of course, the problem is complicated by the motion and impact induced by the paddle; and, to my knowledge, this nonlinear oscillation problem has never been fully investigated. Beatty and Chow [16] have provided a partial solution for the ideal case when the paddle is held fixed and the ball misses the board altogether in the ideal manner suggested in Fig. 19B. We shall not consider this problem here; but the general tools needed to

effect the idealized solution are similar to those that enter the problem of the finite amplitude, free vibration of a mass attached to a rubber string in pure stretch. (See Fig. 19A.) This case is outlined next, and some general characteristics of the oscillation are described.

A neo-Hookean rubber spring of undeformed length ℓ_o, cross-sectional area A_o and fixed at one end is subjected to a homogeneous uniaxial extension by a mass M attached vertically to its other end, as shown in Fig. 20. Let $\ell(t)$ denote the deformed length of the spring at time t; then $\lambda(t) \equiv \ell(t)/\ell_o$ is the amount of stretch at time t. The mass of the spring is assumed negligible compared with M, as usual, so that its motion and the effects of waves propagating in the spring itself may be ignored. The influence of these continuum effects on the finite motion of M is an unsolved problem. Of course, if the spring is a rubber band or strip, compression states are not allowed; this gives rise to the special paddle ball problem mentioned briefly above in Fig. 19B.

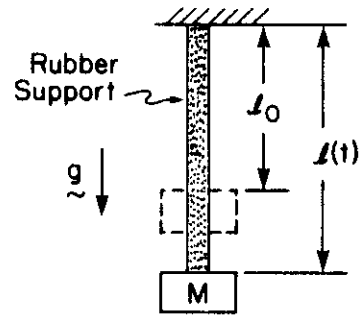

Fig. 20: Finite Oscillations of a Mass on a Rubber Spring.

Since the only forces that act on M are gravity and the hyperelastic spring force, the system is conservative with constant total energy E given by

$$E = \frac{1}{2} M\ell_o^2 \dot{\lambda}^2 + \ell_o \int_{\lambda_o}^{\lambda} T(\lambda)\, d\lambda - Mg\ell_o(\lambda - \lambda_o). \qquad (3.1)$$

Here g denotes the local apparent acceleration of gravity, a dot denotes differentiation with respect to time, and $\lambda_o = \lambda(0)$ is the initial stretch at which the initial "speed" is $v_o = \dot{\lambda}(0)$. Use of (2.3) in (3.1) yields the speed of the mass M supported by a neo-Hookean spring:

$$\dot{\lambda}(t) = v(t) = \pm \left\{ -\frac{2g\kappa}{\ell_o\lambda} \left[\lambda^3 - \frac{\lambda^2}{\kappa} - \frac{V\lambda}{\kappa} + 2\right] \right\}^{1/2} \qquad (3.2)$$

for $\lambda \in [\alpha,\beta]$. The energy constant V in (3.1) is defined by

$$V = V(\lambda_o, v_o) \equiv \frac{\ell_o v_o^2}{2g} + \kappa(\lambda_o^2 + 2\lambda_o^{-1}) - \lambda_o, \qquad (3.3)$$

and $\kappa \equiv A_o E/6Mg$. Hence, the time required for M to move from λ_o to $\lambda(t)$ follows from integration of (3.2) in which the appropriate sign is to be used:

$$t = \pm \int_{\lambda_o}^{\lambda} \frac{d\lambda}{v(\lambda)}. \qquad (3.4)$$

Thus, in a periodic motion between the two admissible extreme stretch states $\lambda(t_1) = \alpha$ and $\lambda(t_2) = \beta > \alpha$ defined by the physical condition that the speed $v(\lambda)$ must vanish at these extremes, the periodic time of the finite amplitude, free vibration of M, defined by $\tau \equiv 2(t_2 - t_1)$, is given by

$$\tau = 2 \int_{\alpha}^{\beta} \frac{d\lambda}{v(\lambda)}. \qquad (3.5)$$

It is seen from (3.2) that (3.4) is a general elliptic integral; hence, the motion is indeed periodic. The standard form may be found by use of the transformation [15-16]

$$\phi(\lambda) \equiv \sin^{-1}\left[\frac{\beta(\lambda - \alpha)}{\lambda(\beta - \alpha)} \right]^{1/2} \text{ so that } \lambda = \alpha[1 + n \sin^2\phi]^{-1}, \qquad (3.6)$$

in which $0 \leq \phi \leq \pi/2$ and the integral parameters are defined by

$$n \equiv \frac{\alpha - \beta}{\beta}, \quad k^2 \equiv \frac{\gamma(\beta - \alpha)}{\beta(\alpha + \gamma)}, \quad 0 < k < \sqrt{-n} < 1, \; \alpha\beta\gamma = 2. \qquad (3.7)$$

When this is done, it turns out that (3.4) is given by

$$t = \pm \frac{\tau^*}{2} [\Lambda(\phi;n,k) - \Lambda(\phi_o;n,k)] \qquad (3.8)$$

in which $\Lambda(\phi;n,k)$ identifies the Heuman Λ-function [15, 17], $\phi_o \equiv \phi(\lambda_o)$ is given by $(3.5)_1$, the scale period $\tau^* \equiv \tau_o/\sqrt{k}$, and the sign is appropriately chosen as noted before. It is seen from (3.6) that for $\lambda_o = \alpha$, $\phi_o = \phi(\alpha) = 0$ and $\phi(\beta) = \pi/2$. Since

the Λ-function has the properties

$$\Lambda(0;n,k) = 0, \quad \Lambda(\tfrac{\pi}{2};n,k) = \Lambda_o(\xi;k) \tag{3.9}$$

in which $\xi \equiv \sin^{-1}[(1 + k^2/n)\div(1 - k^2)]^{1/2}$. It follows that the periodic time has the simple, elegant form

$$\tau = \tau^* \Lambda_o(\xi;k) \tag{3.10}$$

expressed in terms of Λ_o, the tabulated complete Λ-function [17].

It follows from these relations that the finite amplitude, free vibrational period (frequency) of a neo-Hookean oscillator is always less (greater) than the period (frequency) of a linear spring oscillator having the same constant stiffness $k_o = AE/3\ell_o$; that is, $\tau < \tau^*$. More precisely, for $\beta \in (0,\pi/2)$ and for all $k \in (0,1)$, the period τ, hence the frequency p, is bounded as follows:

$$2\beta/\pi < \tau/\tau^* = p^*/p < \sin\beta. \tag{3.11}$$

This is an easy consequence of the properties of the complete Λ-function

It may be shown that the mass oscillates asymmetrically about its equilibrium state. We may recall that a universal property of every linear oscillator is that the dynamical deflection always is exactly twice the static deflection. It turns out that, unlike the linear oscillator in a vertical vibration starting from its undeformed rest state, the magnitude

of the dynamic deflection for a rubber spring suspension support always is larger than twice the static deflection. These features are evident in Fig. 21.

With these results, we now have a better handle on the paddle ball problem, which remains unsolved. We leave this for another place, and turn next to a much simpler problem that has a useful application in life science. The frequency relation for small amplitude motions superimposed on a finitely deformed static state, as illustrated in Fig. 20C, will be described next.

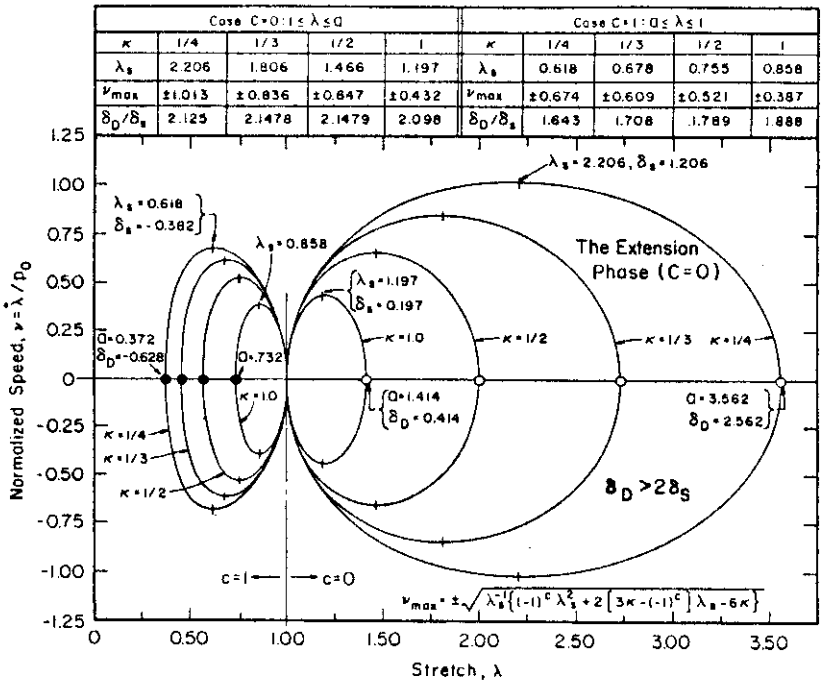

Fig. 21 Phase Plane Graph of the Finite Amplitude Periodic Motion of a Mass Attached to a Neo-Hookean Spring for Various Values of κ and Initial Data $\lambda_0=1$, $v_0=0$. See [12]

Characteristics of the Motion:

1. The mass oscillates asymmetrically about its equilibrium state λ_S.
2. The dynamic deflection from the undeformed rest state is always larger than twice the static deflection. For a linear oscillator, $\delta_D=2\delta_S$ always.

3.2. Small Oscillations Superimposed on an Equilibrium State

Let us suppose that a small displacement $\delta(t)$ is superimposed on an assigned finite static deformation λ_S of the spring so that $\lambda(t) = \lambda_S + \delta(t)$. Substituting this relation into (3.2), retaining only terms to the second order in δ, and then differentiating the result with respect to time, we obtain the differential equation for the small amplitude oscillations of the mass superimposed on an initial finite static stretch of the spring; namely, $\ddot{\delta} + p^2(\lambda_S)\delta = 0$, wherein the small amplitude circular frequency is identified by

$$p(\lambda_S) = p_o \left[\frac{\lambda_S^3 + 2}{\lambda_S(\lambda_S^3 - 1)} \right]^{1/2}. \tag{3.12}$$

The static stretch λ_S is determined by the equilibrium condition

$$\lambda_S^3 + \frac{1}{2\kappa}\lambda_S^2 - 1 = 0. \tag{3.13}$$

Of course, (3.13) has at most one positive solution. An important result follows [15]: Equation (3.12) is a universal relation valid for every neo-Hookean material independently of its elastic modulus; hence, no small amplitude longitudinal oscillation test can distinguish one neo-Hookean material from any other. On the other hand, if (3.12) is not satisfied in every superimposed small amplitude, uniaxial motion of an isotropic, incompressible material, that hyperelastic material can not be modeled as a neo-Hookean material.

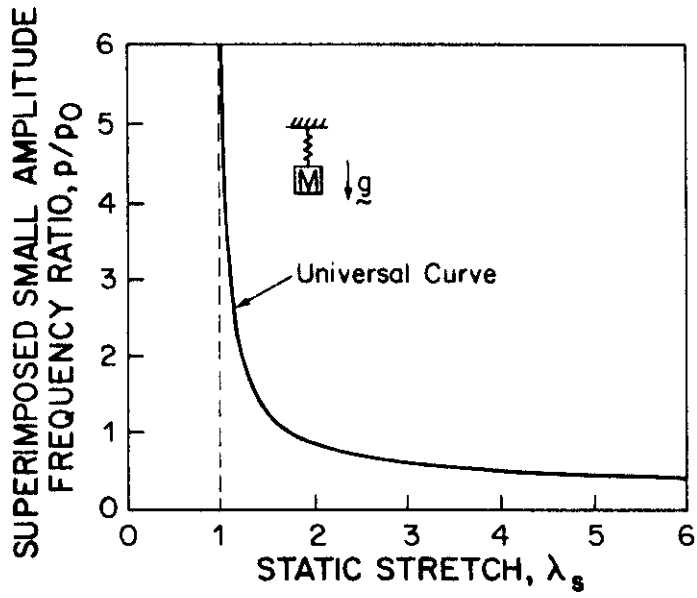

Fig. 22: Universal Frequency Ratio vs. Equilibrium Stretch for Small Amplitude Oscillations Superimposed on a Finite Static Stretch of any Neo-Hookean Spring-Mass Support System. The Frequency Ratio Decreases with Increasing Static Stretch. See [15].

The graph of the universal function (3.12) for the extension case is shown in Fig. 22. If we imagine in Fig. 19C that the ball is loaded statically by a weight W and given a small initial longitudinal disturbance, the frequency of the small amplitude oscillation may be readily counted and timed with the aid of a stopwatch. Suppose next that the weight is doubled and then tripled, and so forth, and the frequency is measured as before. It will be observed that the small amplitude frequency will decrease nonlinearly as the load is increased, that is, as the static stretch is increased. It is seen in Fig. 22 that the universal function (3.12) predicts this nonlinear frequency effect very nicely. Of course, materials that are not neo-Hookean in their response necessarily will behave somewhat differently. This will be seen in the next section wherein some experimental results having application in biology are reviewed.

3.3. Experimental Results: An Application to Life Science

Lawton and King [18] have shown that the universal relation (3.12) describes nicely the small amplitude, free vibrational frequency response curves obtained from test data for certain unfilled gum rubber strips when the static stretch is not greater than 2 to 2.5, approximately. Their data are shown in Fig. 23. All the experimental curves lie above the universal graph (3.12); and for small deformations λ_s near unity, the data share good agreement with the theory. But for larger deformations, there is considerable discrepancy from the monotonic decreasing behavior

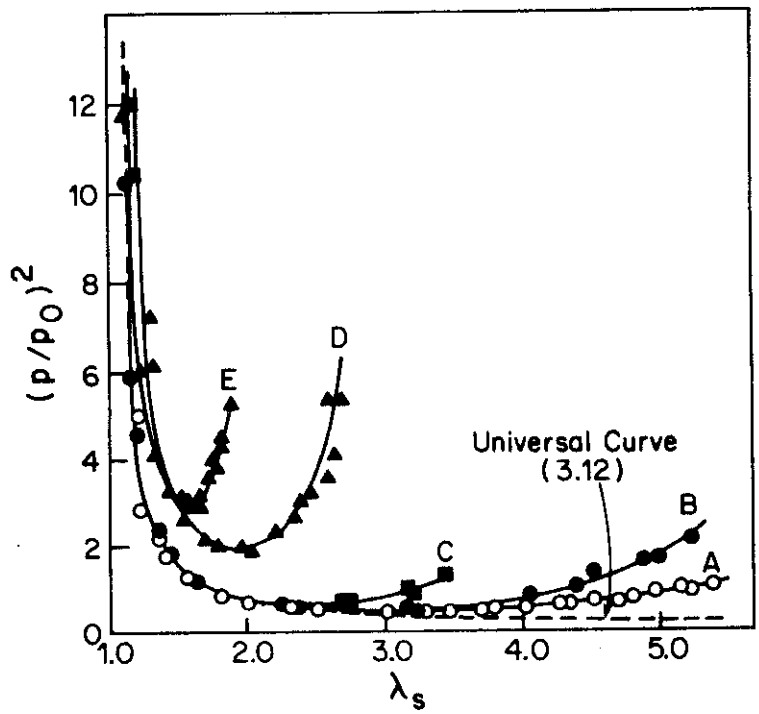

Fig. 23: Experimental frequency response curves of Lawton & King [18]. (A) Gum stock with medium sulfur content, (B) Gum stock with high sulfur content, (C) Strip from a household rubber band, (D) Gum stock A with channel black filler, (E) Circumferential strip of human thoracic aorta (21years). Universal frequency response curve (3.12) is plotted as a dotted line.

characterized by the universal curve. For the gum rubber specimens A, B, and D, the departure for the ideal case widens as the material stiffness is increased by additional sulfur and filler content. The data exhibit distinct minima, the frequency decreasing with increasing static stretch until a certain critical stretch is attained, after which the frequency increases with the stretch. The cause of this behavior is unknown, but it seems clear from the data that the minimum in the frequency response curve is affected by the stiffness. As the material stiffness increases, the corresponding critical stretch decreases and the minimum in the frequency response curve becomes sharper and moves upward and closer to the frequency axis.

Data for an aortic strip cut from the thoracic region of a 21-year old male post mortem shows greater stiffness than any of the rubber materials studied. The affect of aging on males may be seen in Fig. 24 in which the response from an aortic strip

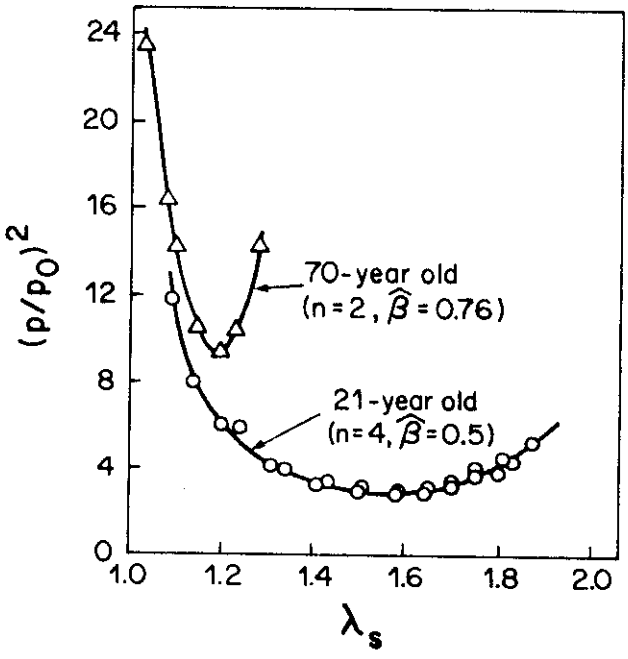

Fig. 24: Small Amplitude Frequency Response vs. Static Stretch Showing the Affect of Aging on the Frequency Response of Male Aortic Tissue. See [18].

taken from the cadaver of a 70-year old male is compared with the aortic strip from the 21-year old male. It is seen that the old aorta is stiffer than the young one, which may be expected intuitively. I would suggest that it is not much different for women either. This simple test, therefore, supports the conclusion [18] that aging arterial walls may lose their extensibility due to increased interchain bonding and deposition of filler-like particles. I think this effect is known more commonly as **hardening of the arteries**.

The discrepancy between the test data and the universal neo-Hookean prediction may be resolved to a considerable, though not completely satisfactory degree by use of the more sophisticated James-Guth model. It may be shown that the frequency of the superimposed small vibration for the James-Guth continuum (2.5) is determined by the rule

$$p(\lambda_S) = p_o \left\{ \frac{\hat{\beta}[2\lambda_S^3 D(\eta) + D(\mu)] + 3\lambda_S^{1/2} L^{-1}(\eta)}{2[\lambda_S^3 L^{-1}(\eta) - \lambda_S^{3/2} L^{-1}(\mu)]} \right\}^{1/2}, \tag{3.14}$$

in which

$$\hat{\beta} \equiv \frac{1}{\sqrt{n}}, \quad \eta \equiv \hat{\beta}\lambda_S, \quad \mu \equiv \frac{\hat{\beta}}{\sqrt{\lambda_S}}, \tag{3.15}$$

and

$$D(z) \equiv \frac{d}{dz} L^{-1}(z) = \frac{z^2 \sinh^2 z}{\sinh^2 z - z^2}. \tag{3.16}$$

We recall that n is the hypothetical average number of links in

the molecular chain structure; it is a measure of the finite extensibility behavior of rubberlike materials. It happens that equation (3.14) reduces to (3.12) when $n \to \infty$.

The theoretical relation (3.14) as a function of λ_s is shown in Fig. 25 for several values of n. It is seen that the James-Guth model is able to account for the observed minima in the superimposed, small amplitude frequency response curve. In this case, the frequency relation for the superimposed small oscillations is not universal, rather the frequency varies with the elastomeric parameter n, the apparent number of links in the molecular chain structure. In fact, in the curve fitting scheme used by Lawton and King [18], the value of n is selected so that

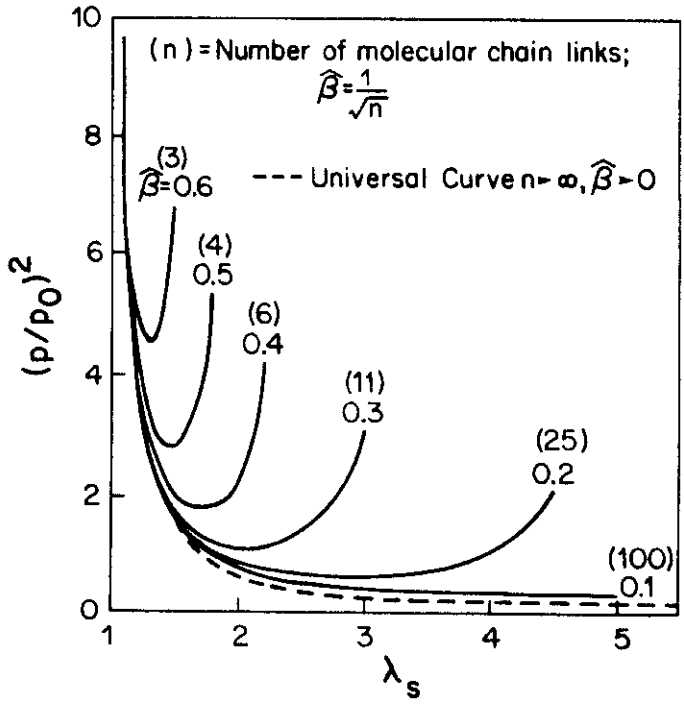

Fig. 25 Theoretical Frequency Response Curves of the James-Guth Model for Values of the Parameter η from 3 to ∞ , or $\hat{\beta}$ from 0 to 0.60. See [18].

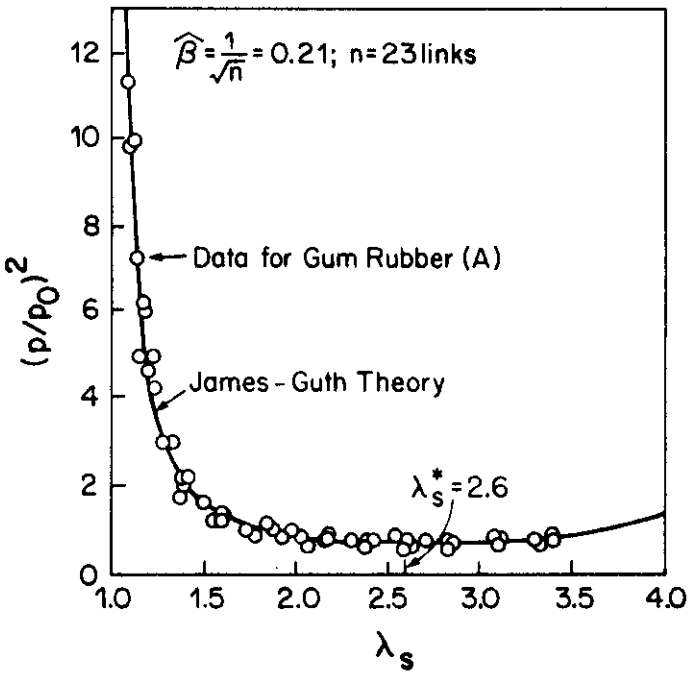

Fig. 26: Experimental Frequency Response Data for Gum Rubber of Low Sulfur Content Compared with James-Guth Model Relation. See [18].

the theoretical curve based on (3.14) has a minimum value of $(p/p_o)^2$ equal to its minimum found in the test. The experimental data shown in Fig. 26 for the gum rubber stock compare favorably with the theoretical result; but for the stiffer, reinforced gum rubber and biological materials, it turned out that the agreement was poor, the data curves being similar but shifted substantially along the stretch axis. The discrepancy for the reinforced gum rubber is shown in Fig. 27. Comparison with the data for the aortic tissues apparently was so poor that the authors chose not to exhibit it. It should be mentioned that the values of n determined in the manner described above are significantly smaller than those found by other static methods; hence, the curve fitting scheme used in [18] may be in serious question. In

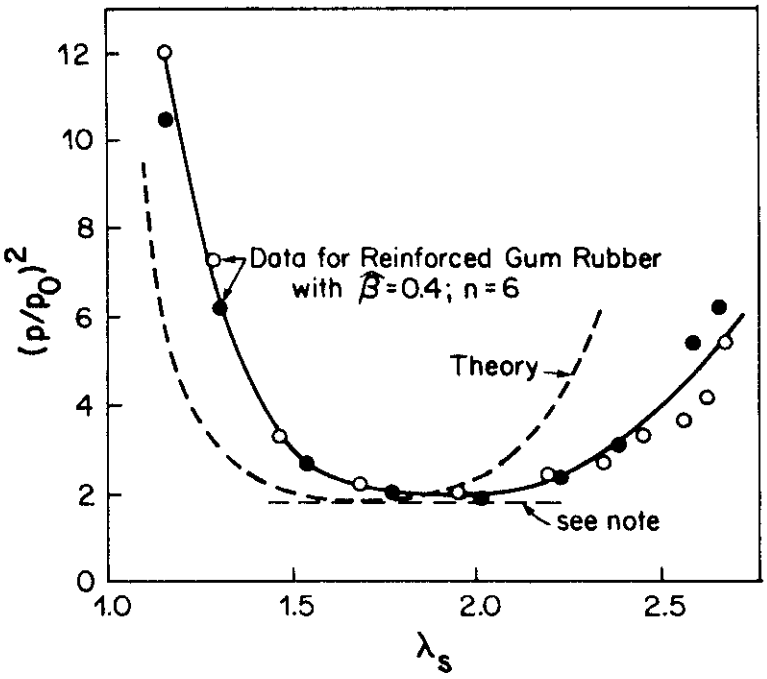

Fig. 27: Frequency Response Curve for Two Specimens of the same Filled Gum Stock. The Result Shows that the Discrepancy Grows with Increased Stiffness.

*Note: n was chosen to produce same minimum value for $(p/p_0)^2$ as determined for the James-Guth Model. See [18].

some rough and unchecked preliminary tests on other elastomers, I have found that for data corresponding to the values of n found in the transverse vibration experiments described earlier, the frequency curves move upward as n decreases, as predicted. However, the curves for the gum and buna-N, which have virtually the same n values, did not lie as close together as I expected they should, based on the transverse vibration tests; rather, there was a considerable horizontal shift in the buna-N data. It is clear that more work, both analytical and experimental, needs to be done toward understanding these basic dynamical phenomena.

CONCLUDING REMARKS

Although the physical principles underlying the operation of the ink jet printer were understood in the 19th century, it was virtually 100 years before this mathematical physics was transformed into useful technology. Moreover, it is evident that the development of the ink jet printer for word processing required the solution of many interdisciplinary dynamical problems in the continuum mechanics of fluids and solids, aerodynamics, acoustics, electrostatics, chemistry and materials science. The foundations of rubber elasticity, on the other hand, are relatively new, and there is need for their further development. While some of the experiments described herein were reported in 1951 and studied on the basis of a theory developed as late as 1943, the analysis of the vibration problems summarized above were published only recently in 1983 and 1984. It was shown that these results are able to explain an unusual acoustical phenomenon, and they have application in materials science of rubberlike materials, including the behavior of biological tissues. It is clear from these few examples that investigation of these problems also demands an interdisciplinary approach. Additional applications presently are being explored. Indeed, their connection with a vehicle stability problem, which evolved from conversation with industrial colleagues following my seminar presentation at the research laboratories of a major tire and rubber manufacturer, currently is under investigation. I had a similar experience concerning the ink jet printer.

I first learned of the ink jet printer invention at a Sunday, summer afternoon piano recital held at the home of an IBM engineer. Our casual shoptalk led to a discussion of a new IBM product, and I was presented with a copy of the July 1976 issue of the Office Products Division Development Newsletter [6] in which this innovative technology was formally introduced. I am easily excited by good ideas; and when suddenly I realized myself the simplicity and basic principle of its operation, I confess that the ink jet printer captured my enthusiasm. A short time thereafter, during the Fall Term 1976, in a manner similar to that sketched above, I presented these elementary ideas for the first time to my undergraduate class in dynamics [19].

I relate this experience because it exemplifies how informal discussion of "hot topics" may be effective in creating interest and enthusiasm for further investigation and search for understanding of new or unexplored areas in applied mathematics, engineering science and technology. Since my arrival at the University last September, I have witnessed in myself and in others at this Institute a parallel experience generated through participation in seven IMA Workshops held throughout the year. By bringing together engineers, physicists, chemists, mathematicians and others, both analysists and experimenters, and by providing a forum for the mutual exchange of ideas and the open discussion among university and industrial researchers of important technical problems, it is conceivable that the use of costly cut and try methods in timely industrial applications may be reduced and the time gap between the discovery and understanding of physical

phenomena and the conversion of this knowledge to useful applications and to technology may be narrowed. To accomplish this goal, mutual interaction between industrial and university personnel must be stimulated and vigorously promoted by both groups. I am pleased to have had the opportunity to help promote this kind of collaboration through presentation of this lecture to both IMA Workshop participants and to our industrial colleagues through the medium of television.

I wish to end with a story told, I believe, in a political speech by John Kennedy. The circumstances are unimportant. The message is clear.

The French General Lautey one day remarked to his gardener that he wished a special variety of tree to be planted, so he directed: "Gardener, plant this tree tomorrow." And the gardener replied; "But, Sir, that variety won't bear fruit for possibly a hundred years." "In that case," replied the General, "plant it today."

Acknowledgement: This work was completed in the course of a research study supported by the National Science Foundation.

References

[1] J.W.S. Rayleigh, On the instability of jets. Proc. London Math. Soc. 10 (1878), 4-13.

[2] J.W.S. Rayleigh, On the capillary phenomena of jets. Proc. Roy. Soc. 29 (1879), 71-79.

[3] W. L. Buehner, The application of ink jet technology to an office product. IBM Office Prod. Tech Rpt. TR 08.092, June 1977.

[4] W.L. Buehner, J.D. Hill, T.H. Williams and J.W. Woods, Application of ink jet technology to a word processing output printer. IBM J. Res. Develop. 21 (1977), 2-9. This entire issue is devoted to various aspects of ink jet printing technology.

[5] R. G. Sweet, High frequency recording with electrostatically deflected ink. Rev. Scient. Instru., Series 2, 36, (1965), 131-136.

[6] L. Kuhn and R.A. Myers, Ink-jet printing, Scient. Amer. 240 (1979), 162-178.

[7] W.L. Buehner, Ink jet printing for the IBM 46/40. Office Products Division Development Newsletter, July 1976.

[8] W.T. Pimbley and H.C. Lee, Satellite drop formation in a liquid jet. IBM J. Res. Develop. 21 (1977), 21-30.

[9] T.J. Baker, The frequency of transverse vibrations of a stretched India rubber cord. Phil. Mag. 49 (1900), 347-351.

[10] V. von Lang, Ueber Transversale Töne von Kaulschukfäden. An. Phys. u. Chem. 68 (1899), 335-342.

[11] J.W.S. Rayleigh, The Theory of Sound, The Macmillan Co., London, 1944.

[12] M.F. Beatty and A.C. Chow, On the transverse vibration of a rubber string. J. Elasticity 13 (1983), 317-344.

[13] L.R.G. Treloar, The Physics of Rubber Elasticity. Clarendon Press, Oxford, 1958, 3nd Ed.

[14] H.M. James and E. Guth, Theory of the elastic properties of rubber. J. Chem. Phys. 11 (1943), 455-481.

[15] M.F. Beatty, Finite amplitude oscillations of a simple rubber support system. Arch. Rational Mech. Anal. 83 (1983), 195-219.

[16] M.F. Beatty and A.C. Chow, Free vibrations of a loaded rubber string. Inter. J. Nonlinear Mech. 19 (1984), 69-81.

[17] C. Heuman, Tables of complete elliptic integrals. J. Math. & Phys. 20 (1941), 127-206. Errata. Ibid. 336

[18] R.W. Lawton and A.L. King, Free longitudinal vibrations of rubber and tissue strips. J. Appl. Phys. 22 (1951), 1340-1343.

[19] M.F. Beatty, The Principles of Engineering Mechanics. Part II: Dynamics - The Analysis of Motion. (To appear).